1-1-2015

Development of electrospun photocatalytic TiO2-polyamide-12 nanocomposites

E Cossich
Universidade Estadual De Maringa

R Bergamasco
Universidade Estadual De Maringa

M T. Pessoa De Amorim
University of Minho

P M. Martins
University of Minho

J Marques
Universidade do Minho

See next page for additional authors

Development of electrospun photocatalytic TiO2-polyamide-12 nanocomposites

Abstract

Titanium dioxide (TiO2) in different forms such as films, fibers or particles are being extensively studied for removal of contaminants from aquatic environments due to its outstanding photocatalytic activity. This work reports the development of TiO_2-polyamide 12 electrospun fiber mats. A systematic study on the influence of electrospun processing parameters on polymer fiber morphology was performed. It was observed that the average fiber diameter is mainly influenced by polymer concentration and average fiber diameters between 404 ± 82 nm and 1442 ± 360 nm were obtained. Polyamide-12 (PA-12) was used as a polymer matrix and electrospun with 0, 10 and 20 wt% of TiO_2. It was observed that the filler does not change the average fiber diameter, being similar to that observed for neat PA-12 fibers processed under the same experimental conditions. The TiO_2 were particles dispensed not only in the bulk of the polymeric matrix but also on the surface of the fibers, especially for the samples with higher filler contents. Neat and nanocomposite electrospun samples show a hydrophobic behavior and a degree of crystallinity of ~25%. The photocatalytic performance of the processed samples was measured by following the degradation capability of a chosen dye, methylene blue (MB). Results show that the nanocomposite samples have a remarkable photocatalytic activity, especially the one with a higher load of TiO_2 particles (20 wt%), with all MB being removed from the solution after 100 min.

Keywords

12, polyamide, tio2, photocatalytic, nanocomposites, electrospun, development

Disciplines

Engineering | Science and Technology Studies

Publication Details

Cossich, E., Bergamasco, R., Pessoa De Amorim, M. T., Martins, P. M., Marques, J., Tavares, C. J., Lanceros-Méndez, S. & Sencadas, V. (2015). Development of electrospun photocatalytic TiO_2-polyamide-12 nanocomposites. Materials Chemistry and Physics, 164 91-97.

Authors

E Cossich, R Bergamasco, M T. Pessoa De Amorim, P M. Martins, J Marques, Carlos J. Tavares, Senentxu Lanceros-Méndez, and Vitor Sencadas

Development of electrospun photocaltalytic TiO_2-Polyamide-12 nanocomposites

E. Cossich[a], R. Bergamasco[a], M.T. Pessoa de Amorim[b], P. M. Martins[c], J. Marques[c], C. J. Tavares[c], S. Lanceros-Méndez[c], V. Sencadas[d,*]

[a] Department of Chemical Engineering, State University of Maringá, 47020-900 Maringá, Brazil

[b] Department of Textile Engineering, University of Minho, 4800-058 Guimarães, Portugal

[c] Centro/Departamento de Física da Universidade do Minho, Campus de Gualtar, 4710-057 Braga, Portugal.

[d] School of Mechanical, Materials and Mechatronics Engineering, University of Wollongong, Wollongong, NSW 2522, Australia

Email: victors@uow.edu.au

Abstract

Titanium dioxide (TiO_2) in different forms such as films, fibers or particles are being extensively studied for removal of contaminants from aquatic environments due to its outstanding photocatalytic activity. This work reports the development of TiO_2-polyamide 12 electrospun fiber mats. A systematic study on the influence of electrospun processing parameters on polymer fiber morphology was performed. It was observed that the average fiber diameter is mainly influenced by polymer concentration and average fiber diameters between 404±82 nm and 1442±360 nm were obtained. Polyamide-12 (PA-12) was used as a polymer matrix and electrospun with 0, 10 and 20 wt% of TiO_2. It was observed that the filler does not change the average fiber diameter, being similar to that observed for neat PA-12 fibers processed under the same experimental conditions. The TiO_2 were particles dispensed not only in the bulk of the polymeric matrix but also on the surface of the fibers, especially for the samples with

higher filler contents. Neat and nanocomposite electrospun samples show a hydrophobic behavior and a degree of crystallinity of ~ 25%.

The photocatalytic performance of the processed samples was measured by following the degradation capability of a chosen dye, methylene blue (MB). Results show that the nanocomposite samples have a remarkable photocatalytic activity, especially the one with a higher load of TiO_2 particles (20 wt%), with all MB being removed from the solution after 100 min.

Introduction

Titanium dioxide (TiO_2) films, fibers or particles are attracting increased attention for photocatalytic applications, in particular for de removal of environmental pollutants related to waste water and polluted air [1]. Usually, if TiO_2 is used in the form of fibers or powder, a post-treatment process is needed to remove the high suspended particles or even clusters, which is a time consuming task [2]. In that sense it is important to develop a photocatalytic membrane with high quantum efficiency, photocatalytic performance, with proper bandgap, strong oxidative ability, high stability in water solution system and easy to remove from the cleaned water after performance.

Electrospinning is a technique used to produce high porous fiber membranes with high permeability, small pore size, high specific surface area, good interconnectivity between the pores, suitable mechanical properties and easy handling and separation from reaction media. Further, it can be up-scaled for mass production of one-by-one continuous micro and nanofibers from various polymers [3, 4].

Krupa *et al.* [5] reported a method to produce core-shell nanocomposites electrospun fibers from three different polymers in the core, namely poly(vinylidene fluoride) (PVDF), poly(vinyl chloride) (PVC) and polysulphone (PSU), the shell being produced

by a solution of 5 wt% of TiO_2 particles suspended in a solution of tetrahydrofuran. The diameter of the produced fibers were in the range 400–800 nm, being the TiO_2 particles disbursed mainly on the surface of the different polymer matrices. It was nevertheless reported that particles tend to form large agglomerates within droplets formed on the fiber due to the surface tension before solvent evaporation. Jaworek *et al.* [6] reported two different methods to incorporate metal oxide particles based on electrospinning and electrospraying. It was similarly reported that the particles do not cover the entire fiber surface and some free space remains between the particle agglomerates. Furthermore, they found that when the electrospray process is performed at 30 and 60 ºC, the number of electrosprayed particles is larger at lower temperatures and the structure is also more densely packed; phenomenon attributed to the higher solvent kinetics that occurs at higher temperature [6].

Electrospun polyamide-6 (PA-6) membranes containing TiO_2 were prepared by Lombardi *et al.* [7]. In their work they also prepared PA-6 membranes by solvent casting with the same filler content and studied the photocatalytic performance by following the degradation of methylene blue (MB) as a function of ultraviolet (UV) irradiation time for both samples with different filler concentrations. Solvent casted samples showed a higher degradation rate performance when compared to the electrospun samples, and such behavior was attributed to the less exposed surface of the photocatalyst in electrospun polymer membranes. Moreover, for polymer films with 20 wt% TiO_2, total degradation of the MB was achieved after 170 min exposure, whereas for electrospun membranes with same filler amount only 70% degradation of total MB was achieved. Further, the authors did not mention the effect of a hydrophilic polymer matrix in the absorption/adsorption of the dye during the photocatalytic measurement.

TiO_2-fluoropolymer electrospun membranes were prepared by He *et al.* [8]. The photocatalyst was immobilized on the surface of the fibers by hydrothermal complex-precipitation, covering the whole polymer surface, giving origin to a core-shell structure with the TiO_2 particles on the fiber surface. The reaction conditions used determined the size and the amount of photocatalyst nanoparticles present on the polymer surface. The degradation of MB solution was used to study the performance of such composite membranes under UV radiation. It was reported that TiO_2-fluorpolymer fiber nanocomposites had a good photocatalytic ability, recycling and stability for applications in environmental remediation, albeit with the full degradation of MB from the solution being achieved for exposure times higher than 150 min [8].

Despite these investigations and large potential applications, there is a lack of a systematic study of how the processing parameters influence electrospun fiber dimensions, and how to properly incorporate TiO_2 nanoparticles into the fiber in order to enhance the photocatalytic activity of the nanocomposites samples.

Polyamide-12 belongs to the polyamide family with longer aliphatic chains, superior properties such as flexibility, resistance to pressure, rigidity, high impact resistance, good mechanical properties (even at higher temperatures), thermal stability, low density, impermeability and outstanding chemical resistance [9]. In this work, TiO_2–PA-12 fiber nanocomposites were prepared by electrospinning. First, it was performed a study of the effect of the processing parameters, such as the applied electrical field, needle inner diameter feed rate, polymer concentration and TiO_2 concentration on the fiber average diameter. We have systematically study the effect of the photocatalyst amount present in the polymer matrix on the photocatalytic activity of the nanocomposite electrospun membranes by following the degradation of methylene blue

upon UV light exposure. It was found that the degradation rate of the blue methylene dye is related to the amount of the photocatalyst present in the fibre matrix.

Experimental

2.1 Materials

Polyamide-12, PA-12, Rilsan^{R}, was produced by Arkema, France. Titanium dioxide (TiO_2, P25 Evonik) was supplied by Evonik. The polymer solutions of PA-12 were dissolved in 1,1,1,3,3,3-Hexafluoro-2-propanol (HFIP, ≥ 99%, Sigma Aldrich) for different polymer concentrations (10, 12, 15 and 18 %wt). Nanocomposites were prepared after ultrasonic dispersion of the TiO_2 powder in an ultrasound bath (Bandelin, model Sonorex Super RK106) during 2 h. The amount of TiO_2 in the solution was selected to result in concentrations between 0 and 20 %wt in the PA-12 matrix. After TiO_2 dispersion, the polymer was added to the solution and dissolved with the help of a magnetic stirrer, at room temperature, until complete dissolution.

2.2 Electrospinning

The polymer solution was placed in a commercial syringe (10 mL) fitted with a steel needle with different inner diameters (between 0.2 to 1.7 mm). Electrospinning was conducted at different applied electric fields (between 0.8 $kV.cm^{-1}$ and 1.4 $kVcm^{-1}$) with a high voltage power supply from *Glassman* (model PS/FC30P04). A syringe pump (from *Syringepump*) was used to feed the polymer solution into the needle tip, at a rate between 0.1 and 4.0 $mL.h^{-1}$ and the electrospun fibers were collected in a grounded collecting plate. The distance between the needle and the collector was kept constant at 15 cm.

2.3 Electrospun fiber membrane characterization

Electrospun fiber membranes were coated with a thin gold layer using a sputter coating (*Polaron*, model SC502), and their morphology was analyzed using scanning electron microscopy (SEM) (Quanta 650 from FEI) with an accelerating voltage of 5 kV. The fiber average diameter and their size distribution was calculated over approximately 40 fibers using SEM images at 5000× magnification and Image J software. Contact angle measurements (sessile drop in dynamic mode) were performed at room temperature in a Data Physics OCA20 device using ultrapure water as test liquid. The contact angles were measured by depositing water drops (3 µL) on the sample surface and analyzed with the SCA20 software. At least 6 measurements in each sample were performed in different membrane locations, and the average contact angle was taken as the result for each sample.

Infrared measurements (FTIR) were performed at room temperature in an Apha FTIR apparatus from Bruker in attenuated total reflectance (ATR) mode from 4000 to 600 cm^{-1}. FTIR spectra were collected after 32 scans with a resolution of 4 cm^{-1}. The measurements were performed at room temperature. Differential scanning calorimetry (DSC) measurements were performed in a Mettler-Toledo DSC28e apparatus at a heating rate of 10ºC.min^{-1}. The samples were cut into small pieces from the membrane central region and placed into 40 µL aluminum pans. All experiments were carried out using nitrogen as purge gas. The degree of crystallinity (X) of the polymer was calculated as:

$$X(\%) = \Delta H_s/\Delta H_0 \quad (1)$$

where ΔH_s is the enthalpy of the sample, and ΔH_0 is the melting enthalpy of a 100 % crystalline PA-12 material ($\Delta H_0 = 209.34$ J/g was used [10]).

The degree of porosity of the membrane was determined by the pycnometer method following the procedure described elsewhere [11]. Briefly, the weight of the pycnometer filled with ethanol was measured and labeled as W_1; the sample with weight W_s was immersed in ethanol. Subsequently, the sample was saturated by ethanol; additional ethanol was added to complete the volume of the pycnometer. Then, the pycnometer was weighted and labeled as W_2; the sample filled with ethanol was taken out of the pycnometer and the residual weight of the ethanol and the pycnometer was labeled as W_3. The porosity of the membrane was calculated according to:

$$\varepsilon = (W_2 - W_3 - W_s)/(W_1 - W_3) \quad (2)$$

The mean porosity of each membrane was obtained as the average of the values determined in three samples.

2.4 - Photocatalytic activity

Photocatalytic oxidation of methylene blue (MB) solution by TiO_2-PA-12 nanocomposite fiber membranes under UV irradiation was used to evaluate the photocatalytic activity of the samples. Tests were performed in 3.5×3.5 cm^2 electrospun samples (with a thickness of ~70 μm) placed in the inside wall of a quartz cell (40mm × 40mm × 10 mm) and filled with MB aqueous solution (13 mL, 10^{-2} mM, pH = 6.8). Subsequently, the sample immersed in MB solution was placed in a dark chamber during 30 min, to reach an adsorption–desorption equilibrium of the MB. Finally, the quartz cell was irradiated with a high power LED source (Thorlabs, 700 mA) with an excitation peak at 365 nm (UV-A).The incident radiation over the sample was measured with a photo-radiation meter and the average values were around 5mW·cm^{-2} [12]. The

absorbance of the MB was monitored at intervals of 2 min using a spectrophotometer (ScanSpecUV-Vis, ScanSci) in the range of 300 to 900 nm. The rate of photodegradation of MB was analyzed by monitoring the intensity variation of the main absorption peak at 662 nm.

The MB degradation in aqueous solution fits to a pseudo-first-order reaction, Langmuir–Hinshelwood model, which can be expressed by [13]:

$$\ln(C/C_0) = kt \quad (3)$$

where C represents the concentration of the dye at the time t and k is the first-order rate constant of the reaction.

Results and Discussion

Effect of electrospinning parameters on fiber and fiber mat morphology

Electrospinning parameters usually have influence in fiber morphology, with several processing parameters including initial polymer solution, concentration, polymer molecular weight, affecting the final fiber diameter. Moreover, jet formation and solvent evaporation kinetics are infuenced by polymer feed rate, needle inner diameter, applied electric field and processing temperature [4]. Collecting procedure not only influences fiber orientation but also mean fiber diameter, especially if a dynamic collector is used such a drum collector, due to the rotational speed that promotes an adittional mechanical stretch to the fibers, leading to a deacrease of the mean fiber diameter [14, 15].

In the present work, electrospun fibers of PA-12 were obtained by dissolving the polymer in HFIP and the experimental processing parameters were systimatically changed in order to study their influence in polymer fiber formation, morphology and average diameter. The obtained electrospun membranes showed a random orientation

with smooth and cilindrical shape fibers and without the present of beads (Figure 1). Figure 1 shows represenative scanning electron microscopy images of the PA-12 fibers obtained under different experimental conditions.

Figure 1

The applied electric field is a key parameter of the electrospinning process. The formation of thin fibers is mainly achieved by the stretching and acceleration of the jets promoted by the high electric field [14, 16]. It has been generally reported that the diameter of the fibers becomes gradually smaller with increasing applied electrical field (E) [17-20]. Further, increasing E also affects other processing parameters such as jet traveling time, which has the opposite effect on the fiber diameter leading to a broader fiber diameter distribution [14, 15, 18] through the formation of fiber branches, with smaller jets being ejected from the primary one, which can be comparable to the ejection of an initial jet from the surface of a charged droplet [3].

In the present work, it was observed that applied electric field, needle inner diameter and polymer flow rate variation does not influence significantly fiber mean diameter (Figure 2a and 2b). A broader fiber distribution was observed for the more extreme processing conditions, which can be related to the increase of polymer solution available at the needle tip giving origin to the formation of fiber branches, with smaller jets being ejected from the primary one (Figure 2c).

Solution viscosity also plays an important role in the electrospinning process promoting polymer chain entanglement, preventing the driven jet from breaking up during the travel between the needle and the ground collector. If the polymer concentration is lower, insufficient chain entanglement occurs, leading to the presence of beads among the fiber membrane. Although, if the polymer concentration is high, it will result in larger polymer chain entanglements within the solution, which often leads to needle

clogging. In the present work, polymer concentrations below 12 wt% resulted in the presence of the beads among the polymer membrane (data not shown) and polymer concentrations above 18 wt% lead to needle clogging just after the process started due to the high solution viscosity. Polymer concentrations between 12 and 18 wt% resulted in the presence of smooth fibers (Figure 1) and it was observed that increasing PA12 concentration in the solution leads to an almost linearly increase on average fiber diameter and to a broader fiber diameter distribution (Figure 2d). This behavior is related to the higher chain entanglement promoted by higher polymer concentrations (figure 2d).

Figure 2

As a conclusion, the PA-12 fiber electrospun membranes are mainly influenced by polymer concentration. In that sense, polymeric nanocomposites electrospun membranes were processed based in the results obtained for neat polymer. The influence of the TiO_2 concentration in the nanocomposites electrospun fiber diameter was evaluated, keeping constant the polymer concentration (12 wt%), applied electric field (1.2 $kV.cm^{-1}$), needle inner diameter ($\emptyset = 0.5\ mm$), distance between the needle and the grounded collector (15 cm) and flow rate (0.2 $mL.h^{-1}$) (Table 1). In general, the electrospun TiO_2-PA-12 membranes showed a smooth fiber surface with a random distribution, similar to the neat polymer with an average fiber diameter of 404±82 nm (Figure 3). For the nanocomposite samples, some filler clusters are observed among the polymeric electrospun matrix due to the large ceramic content for the given average fiber diameter, but the photocatalyst nanoparticles do not cover the entire fiber surface, even for higher TiO_2 concentrations (Figure 3d). Similar results were observed for electrospun fibers from $BaTiO_3$/poly(vinylidene fluoride-trifluorethylene) (PVDF-TrFE) in which the increase of filler content does not affect the polymeric fiber mean

diameter, but some clusters of $BaTiO_3$ were found on the surface of the PVDF-TrFE [21]. Furthermore, it was reported that the incorporation of NaY zeolite in electrospun poly(vinylidene fluoride) (PVDF) fibers lead to an increase of the average fiber diameter and even for filler concentration as small as 4 wt%, some clusters were also observed in the surface of the polymeric fiber matrix [22].

Figure 3

The average water contact angle (WCA) revealed that neat polymer and the nanocomposite electrospun fiber mats present a strong hydrophobic behaviour (insets of Figure 3a-b-c) and the incorporation of the filler does not affect significantly electrospun mats wettability, being the WCA of ~ 136º (Figure 4).

Figure 4

Infrared spectroscopy in attenuate total reflectance (FTIR-ATR) was used to monitor variations at a molecular level that might occur due to the processing conditions of PA-12 and TiO_2-PA-12 nanocomposite fiber mats (Figure 5a). The characteristic FTIR spectra obtained for the samples processed at different applied electric fields are quite similar: no vibrational modes are totally suppressed and no new modes seems to appear due to varying processing parameters (Figure 5a), that is, the structure and the crystalline phase of the PA-12 remains the same, regardless electrospinning conditions.

The characteristic polymer absorption bands appear at 3300 cm^{-1}, assigned to the N-H stretch of amide A, asymmetric and symmetric CH_2 stretching vibrations are observed at 2919 and 2850 cm^{-1}, respectively. The vibrational modes of amide I and amide II appears at 1636 (C=O stretching) and 1542 cm^{-1} (C-N stretching and C=O in plane bending), respectively (Figure 5a) [23].

Figure 5b shows non-isothermal DSC thermograms obtained for neat and nanocomposite electrospun samples at a heating rate of 10ºC.min^{-1}, from 40 up to 200

ºC. All samples showed the same profile, with a glass transition around 50 ºC, which is not affected by the processing parameters or the presence of the filler. In addition, an endothermic peak above 160 ºC was registered, which is associated to the melting of the crystallites. Neither the melting peak temperature, the onset temperature nor the shape of the peak shows significant variations between samples, even for the nanocomposites (Figure 5b). It was also observed the appearance of a small exothermic shoulder prior to melting especially for neat PA-12 electrospun samples, which is probably due to a cold crystallization process during the heating of the PA-12 fibers (Figure 5b) [10, 23]. The degree of crystallinity was calculated according to Equation 1 and all samples showed similar crystalline content around 25 %.

Figure 5

Photocatalytic Activity Evaluation

In order to study the photocatalytic activity of nanofibers, degradation of MB in aqueous solution under UV irradiation was evaluated at room temperature. To validate comparisons of the photocatalytic assays, the tested fiber membranes presented similar thickness (~70 μm) and porosity (~78%). As depicted in Figure 6, the pristine PA-12 membrane fibers does not show a significant absorption/adsorption of MB during 30 minutes in the dark, owing to the hydrophobic feature of the membrane. During UV exposure, no significant decrease of the absorbance was observed, indicating that no absorption/adsorption and/or degradation of MB occurred (Figure 6), which probably due to the hydrophobic nature of the polymer matrix, as shown in figure 3 and 4. Further, for composite electrospun samples it is evident that there was degradation of MB, especially for the sample with 20 wt% TiO_2: a larger interaction of the dye and the inorganic fillers, due to an overall larger TiO_2 content, implies a faster degradation mechanism. Due to the hydrophobic nature of the polymer matrix (figure 3 and 4), the

degradation of the blue dye was only possible due to the interaction between the MB and the photocatalyst. The reaction rate of the nanocomposite samples was obtained through Equation 3, by fitting the data of Figure 6. As expected, k increases with increasing filler content present in the fibers (Table 1), and after 100 minutes of UV exposure, 98% of the MB present in the solution is completely removed.

Figure 6

In this sense, the efficient performance of the as produced photocatalytic fibers is mainly achieved by the synergetic combination of an highly porous structure and a high surface area yielded by the fiber microstructure, which efficiently favours the adsorption-migration-photodegradation process during degradation of MB using TiO_2-PA-12 fiber nanocomposites. In the adsorption-migration-photodegradation process, the MB is probably adsorbed by the polymer fibers, and then migrated to the TiO_2 nanoparticles, and finally degraded by TiO_2 catalyst under UV radiation [8]. Additionally, the MB solution became completely colourless after 100 min of irradiation.

Table 1

The use of MB as a dye to study the potocatalytic is a common procedure and in this way conclusions can be made concerning the efficiency of the built system and on the functionalysation method used. Table 2 shows results reported in literature concerning the use of polymer elctropsun fibres with different TiO_2 particles for the aforementioned prurposes. Nevertheless, comparison is not always staightfoward due to the different conditions used to measure samples perfomance in the MB dye removal.

Photocatalysis mechanism on surface TiO_2 particles is the same ofr any semiconductor catalyst; however photocatalyst acessibility of the dye determine the degradation rate of the process. In the present work, fibres with an average diameter of 404±82 nm, loaded

with 20 wt% of photocatalyst nanoparticles originate clusters bigger than fiber diameter (figure 3), offering a much higher specific surface area than solvent casting membranes or conventional fibres, and consequently those particles will be directly exposed to the dye, leading to an enhanced interaction of the UV light with the nanoparticles, enhancing their photocatalyst activity, resulting in a faster degradation of MB dye.

Table 2

Conclusions

Polyamide 12 electrospinning processing parameters were systematically studied. It was observed that the average fiber diameter is mainly influenced by polymer concentration and average fibers between 404 ± 82 nm and 1442 ± 60 nm were obtained. Moreover, TiO_2 – PA-12 nanocomposite electrospun fibers with 10 and 20 wt% of photocatalyst were also processed and it was observed that the filler does not modify the average fiber diameter, being similar to the observed for neat PA-12 fibers processed in same experimental conditions. Furthermore, the filler particles are dispersed not only in the bulk of the polymeric matrix but also on the surface of the fibers, especially for the samples with higher filler contents. Neat and nanocomposite electrospun samples show a strong hydrophobic behavior. The electrospinning process does not influence polymer matrix characteristics, and samples with ~ 25% crystallinity were obtained.

The photocatalytic performance of the processed samples was measured using methylene blue as target molecule. The results obtained show that the nanocomposite samples have a remarkable photocatalytic activity, especially the one with higher a TiO_2 content (20% wt.), with all MB being removed from the solution after 100 min.

Acknowledgments

This work was supported by FEDER through the COMPETE Program and by the Portuguese Foundation for Science and Technology (FCT) in the framework of the Strategic Project PEST-C/FIS/UI607/2014, and CNPq (Conselho Nacional de Desenvolvimento Científico e Tecnológico – Brazil). The authors also thank funding from Matepro –Optimizing Materials and Processes", ref. NORTE-07-0124-FEDER-000037", co-funded by the "Programa Operacional Regional do Norte" (ON.2 – O Novo Norte), under the "Quadro de Referência Estratégico Nacional" (QREN), through the "Fundo Europeu de Desenvolvimento Regional" (FEDER). PM thanks the FCT for the, SFRH/BD/98616/2013 grant. VS and SLM also thank support from the COST Action MP1206 "Electrospun Nano-fibers for bio inspired composite materials and innovative industrial applications". VS thanks the EIS Faculty at UOW for the starting grant.

References

[1] A. Fujishima, K. Honda, Nature, 238 (1972) 37-38.
[2] R. Nirmala, H.Y. Kim, R. Navamathavan, C. Yi, J.J. Won, K. Jeon, A. Yousef, R. Afeesh, M. El-Newehy, Ceramics International, 38 (2012) 4533-4540.
[3] S. Ramakrishna, K. Fujihara, W. E. Teo, T. C. Lim, Z. Ma, Introduction to electrospinning and nanofibers, World Scientific, Singapure, 2005.
[4] W.E. Teo, S. Ramakrishna, Nanotechnology, 17 (2006) R89.
[5] A. Krupa, A. Jaworek, S. Sundarrajan, D. Pliszka, S. Ramakrishna, FIBRES & TEXTILES in Eastern Europe 20 (2012) 25 - 27.
[6] A. Jaworek, A. Krupa, M. Lackowski, A.T. Sobczyk, T. Czech, S. Ramakrishna, S. Sundarrajan, D. Pliszka, Journal of Physics: Conference Series, 146 (2009) 012006.
[7] M. Lombardi, P. Palmero, M. Sangermano, A. Varesano, Polymer International, 60 (2011) 234-239.
[8] T. He, Z. Zhou, W. Xu, F. Ren, H. Ma, J. Wang, Polymer, 50 (2009) 3031-3036.
[9] T. McNally, W. Raymond Murphy, C.Y. Lew, R.J. Turner, G.P. Brennan, Polymer, 44 (2003) 2761-2772.
[10] J.K.W. Sandler, S. Pegel, M. Cadek, F. Gojny, M. van Es, J. Lohmar, W.J. Blau, K. Schulte, A.H. Windle, M.S.P. Shaffer, Polymer, 45 (2004) 2001-2015.
[11] C.M. Costa, L.C. Rodrigues, V. Sencadas, M.M. Silva, J.G. Rocha, S. Lanceros-Méndez, Journal of Membrane Science, 407–408 (2012) 193-201.

[12] J. Marques, L.F. Oliveira, R.T. Pinto, P.J.G. Coutinho, P. Parpot, J.R. Gois, J.F.J. Coelho, F.D. Magalhães, C.J. Tavares, International Journal of Photoenergy, 2013 (2013) 9.
[13] J. Yu, G. Wang, B. Cheng, M. Zhou, Applied Catalysis B: Environmental, 69 (2007) 171-180.
[14] C. Ribeiro, V. Sencadas, J.L.G. Ribelles, S. Lanceros-Méndez, Soft Materials, 8 (2010) 274-287.
[15] R. Clarisse, et al., Science and Technology of Advanced Materials, 12 (2011) 015001.
[16] X.-H. Qin, Y.-Q. Wan, J.-H. He, J. Zhang, J.-Y. Yu, S.-Y. Wang, Polymer, 45 (2004) 6409-6413.
[17] S. Zhao, X. Wu, L. Wang, Y. Huang, Journal of Applied Polymer Science, 91 (2004) 242-246.
[18] K. Gao, X. Hu, C. Dai, T. Yi, Materials Science and Engineering: B, 131 (2006) 100-105.
[19] M.M. Demir, I. Yilgor, E. Yilgor, B. Erman, Polymer, 43 (2002) 3303-3309.
[20] S. Megelski, J.S. Stephens, D.B. Chase, J.F. Rabolt, Macromolecules, 35 (2002) 8456-8466.
[21] J. Nunes-Pereira, V. Sencadas, V. Correia, J.G. Rocha, S. Lanceros-Méndez, Sensors and Actuators A: Physical, 196 (2013) 55-62.
[22] A.C. Lopes, C. Ribeiro, V. Sencadas, G. Botelho, S. Lanceros-Méndez, J Mater Sci, 49 (2014) 3361-3370.
[23] S. Rhee, J.L. White, Journal of Polymer Science Part B: Polymer Physics, 40 (2002) 2624-2640.
[24] H.R. Pant, B. Pant, P. Pokharel, H.J. Kim, L.D. Tijing, C.H. Park, D.S. Lee, H.Y. Kim, C.S. Kim, Journal of Membrane Science, 429 (2013) 225-234.
[25] N. Daels, M. Radoicic, M. Radetic, S.W.H. Van Hulle, K. De Clerck, Separation and Purification Technology, 133 (2014) 282-290.

Figure and Table Captions

Figure 1 – Polyamide 12 electrospun membranes obtained at different processing conditions: a) polymer concentration of 12 wt%, $E = 1kV.cm^{-1}$, feed rate of 0.2 ml.h^{-1} and needle inner diameter of 0.5 mm, b) polymer concentration of 12%, $E = 1kV.cm^{-1}$, feed rate of 0.2 ml.h^{-1} and needle inner diameter of 1.7 mm, c) polymer concentration of 12 wt%, $E = 1kV.cm^{-1}$, feed rate of 4.0 ml.h^{-1} and needle inner diameter of 0.5 mm and d) polymer concentration of 18%, $E = 1kV.cm^{-1}$, feed rate of 0.2 ml.h^{-1} and needle inner diameter of 0.5 mm. All experiments were performed at room temperature.

Figure 2 – Influence of the different electrospinning parameters on PA-12 average fiber diameter and distribution of fiber sizes: a) applied electrical field, b) needle inner diameter, c) polymer feed rate and d) polymer concentration.

Figure 3 - Influence of the different electrospun parameters of TiO_2 – PA-12 average fiber diameter and distribution of fiber size: a) 0 wt% filler, b) 10 wt% filler, c) 20 wt% filler (inset shows a photocatalyst cluster) and d) evolution of fiber average diameter with the incorporation of TiO_2. All samples were obtained with a polymer concentration of 12 wt%, $E = 1kV.cm^{-1}$, feed rate of 0.2 $mL.h^{-1}$ and needle inner diameter of 0.5 mm.

Figure 4 - Influence of the different TiO_2 concentration on average water contact angle (WCA). All samples were obtained with a polymer concentration of 12 wt%, $E = 1kV.cm^{-1}$, feed rate of 0.2 $mL.h^{-1}$ and needle inner diameter of 0.5 mm.

Figure 5 – a) FTIR spectra of PA-12 electrospun membranes obtained for different applied electrical fields for a polymer concentration of 12 wt%, needle inner diameter of 0.5 mm, and a feed rate of 0.2 $mL.h^{-1}$, and b) DSC of electrospun PA-12 electrospun mats: A (0.8 $kV.cm^{-1}$, random fibers), B (0.8 $kV.cm^{-1}$, random fibers), C (0.8 $kV.cm^{-1}$, aligned fibers) and D (20 wt% TiO_2, 0.8 $kV.cm^{-1}$, random fibers).

Figure 6 – Methylene blue photodegradation performance of for PA-12 nanocomposites electrospun membranes

Table 1 – First-order rate constant (k) and degradation level of MB aqueous solution (10^{-5} M, pH = 6.8), for all produces electrospun nanocomposites.

Table 2 – Comparative study on MB removal reported in literature for electrospun membranes functionalized with TiO2 after 120 min under UV irradiation.

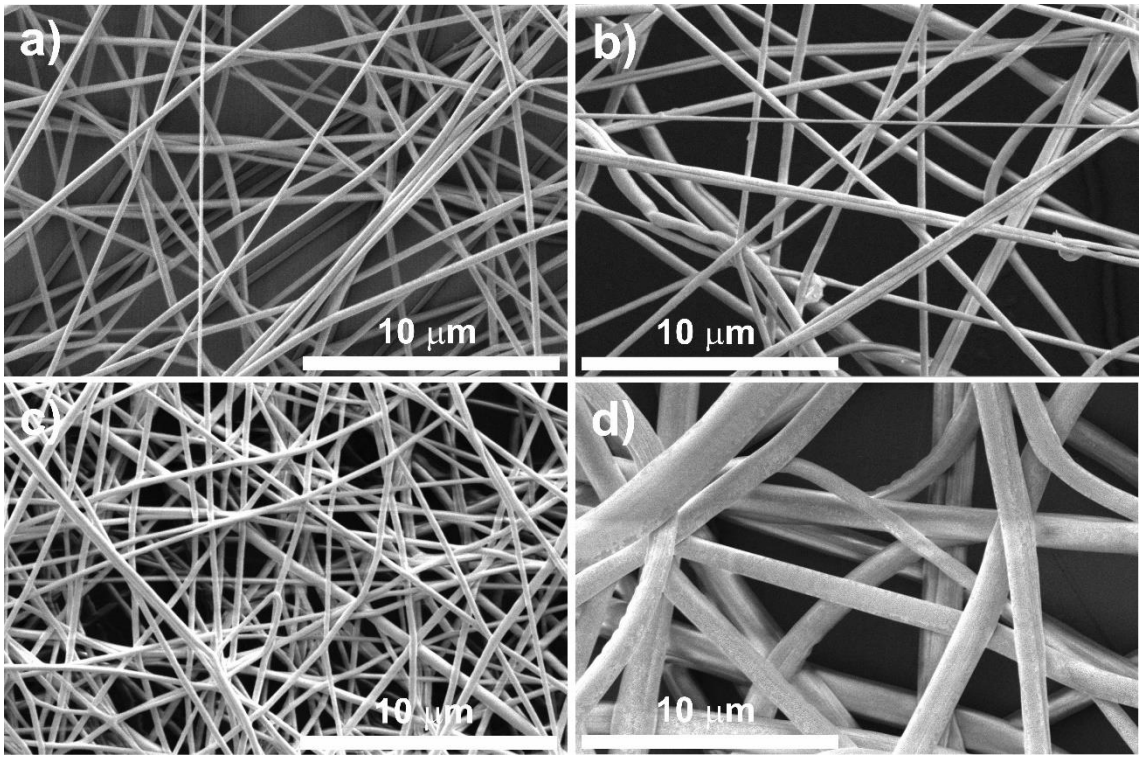

Figure 1

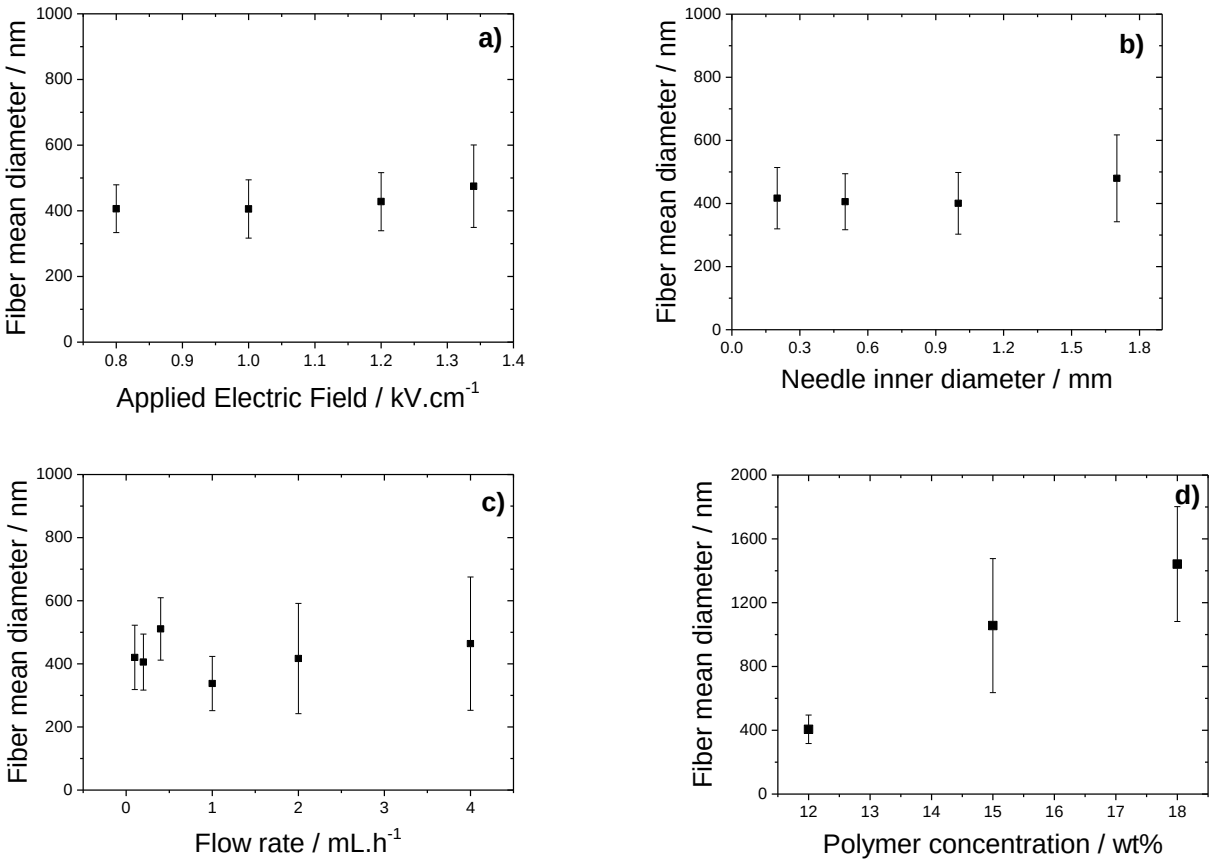

Figure 2

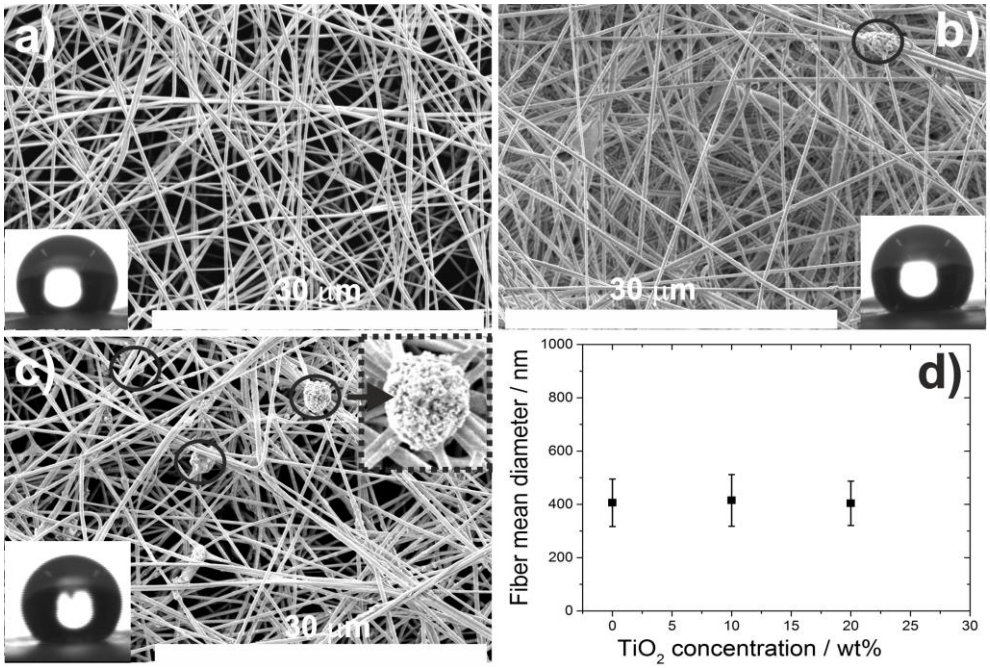

Figure 3

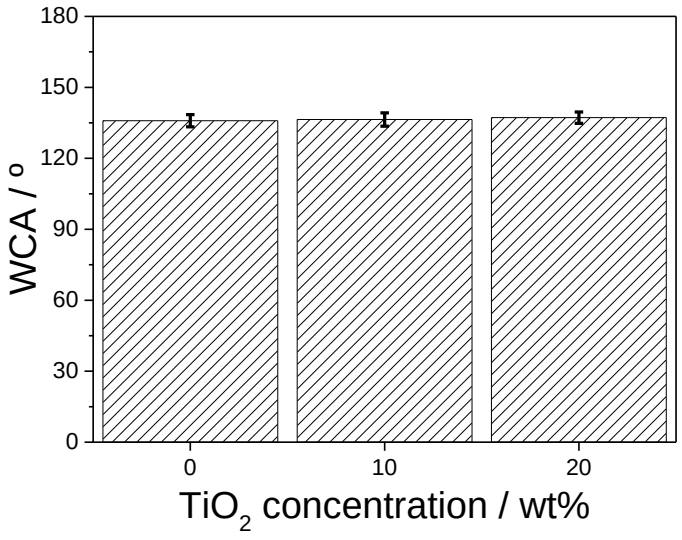

Figure 4

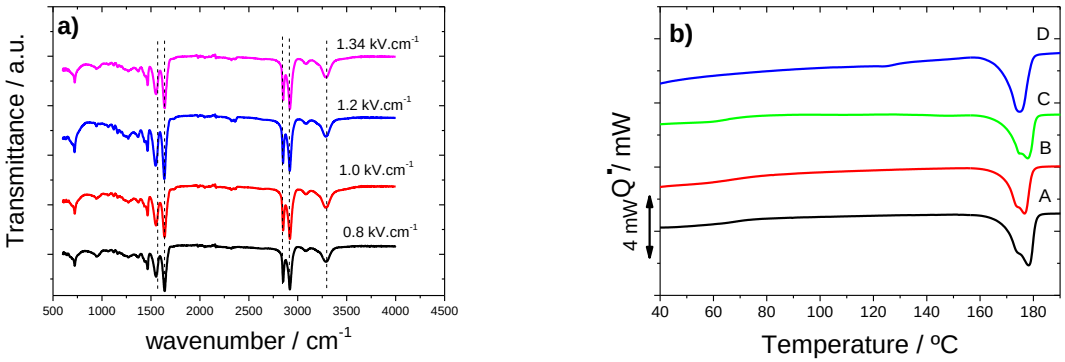

Figure 5

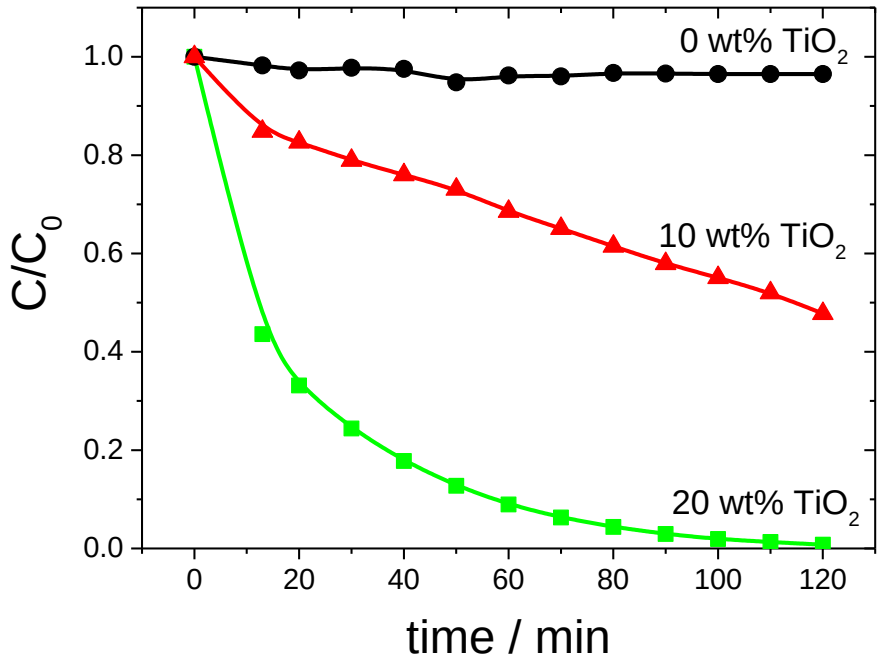

Figure 6

TIO_2 AMOUNT	DEGRADATION RATE	DEGRADATION OF MB SOLUTION AFTER 100 MIN
wt.%	1000/min	%
0	1.9	13
10	4.1	41
20	11.6	98

Table 1

UV LAMP SOURCE POWER	SIZE AND TYPE OF TIO_2	DEGRADATION OF MB AFTER 120 MIN (%)	REFERENCE
2X15 W	10 nm anatase	88	[8]
15 W	21 nm P25	49	[24]
15 W	6 nm	26	
	21 nm P25	84	[25]
5 mW/cm^2	21 nm P25	100	This work

Table 2